ARTICLE IN PRESS

Journal of Hydrology xxx (2010) xxx–xxx

Contents lists available at ScienceDirect

Journal of Hydrology

journal homepage: www.elsevier.com/locate/jhydrol

Quantification of 3-D soil macropore networks in different soil types and land uses using computed tomography

Lifang Luo [a,b], Henry Lin [c,*], Shuangcai Li [d]

[a] US Salinity Laboratory, Riverside, CA 92507, United States
[b] Dept. of Environmental Sciences, University of California, Riverside, CA 92521, United States
[c] Dept. of Crop and Soil Sciences, The Pennsylvania State University, University Park, PA 16802, United States
[d] Dept. of Civil Engineering, The Pennsylvania State University, University Park, PA 16802, United States

ARTICLE INFO

Article history:
Available online xxxx

Keywords:
Computed tomography
Connectivity
Land use
Macropore
Macropore flow
Pore network characterization

SUMMARY

The importance of soil macropores as preferential pathways for water, air, and chemical movement in different soils has long been recognized. However, quantification of complex macropore structures and their relationships to soil types and land uses remains elusive. The objectives of this study were to (1) quantify 3-D macropore networks in intact soil columns using an improved approach and (2) investigate the effects of soil type and land use on soil macropore characteristics. Two soils with contrasting textures and structures (Hagerstown silt loam and Morrison sand) from two land uses (row crop and pasture) were investigated. Intact soil columns, 102 mm in diameter and about 350 mm in length, were taken for each soil type-land use combination. The soil columns were scanned using X-ray computed tomography at a voxel resolution of 0.234 mm × 0.234 mm × 2.000 mm. After reconstruction, characteristics of macropore networks were quantified, including continuous macroporosity change along depth, macropore size distribution, network density, surface area, length density, length distribution, mean hydraulic radius, tortuosity, inclination (angle), and connectivity (path number and node density). The approach we developed provided an improved quantification of complex 3-D macropore networks. The analysis of variance indicated that soil type, land use, and their interaction significantly influenced macroporosity, network density, surface area, length density, node density, and mean angle. The interaction of soil type and land use also influenced mean tortuosity and hydraulic radius. Within the same soil type, the soils under pasture land use had greater macroporosity, length density, and node density than that under row crop, especially in the subsoil. This was due to greater organic matter content and more biota activities in the pasture. Within the same land use, the Morrison sand displayed lower overall macroporosity than the Hagerstown silt loam because of weaker structure and higher amount of rock fragments in the Morrison soil and thus less suited for biota activities. The results from this study provide improved quantitative evaluation of a suite of soil macropore features that have significant implications for non-equilibrium flow prediction and chemical transport modeling in field soils.

© 2010 Elsevier B.V. All rights reserved.

1. Introduction

The importance of macropores as preferential pathways of water, air, and chemicals in the soil has been widely recognized (Beven and Germann, 1982; Lin et al., 2005; Jarvis, 2007). The conductivity of macropores to water flow strongly depends on the 3-D geometry and topology of macropores. Macroporosity, number of macropores, pore length, pore size distribution, continuity, tortuosity, and connectivity are considered as significant characteristics that influence water flow and solute transport through macropores (Perret et al., 2000; Pierret et al., 2002; Bastardie et al., 2003; Peth et al., 2008; Luo et al., 2008). Different types of macropores have distinct geometries and therefore function differently (Lin et al., 1996; Luo et al., 2008). Soil type and land use are among the main factors influencing macropore characteristics (e.g., Gantzer and Anderson, 2002; Zhou et al., 2008; Udawatta et al., 2008; Mooney and Morris, 2008).

Reconstruction, visualization, and quantification of 3-D macropore networks are essential to correlating macropore characteristics to their physical, chemical, and biological functions and to predicting their dynamics under different land uses. The tradition methods, such as thin-sections, have limited ability to observe 3-D macropore geometry and topology. With advances in imaging techniques, X-ray computed tomography (CT) has become attractive for non-destructively observing soil structure including

* Corresponding author. Tel.: +1 814 865 6726; fax: +1 814 863 7043.
E-mail address: henrylin@psu.edu (H. Lin).

0022-1694/$ - see front matter © 2010 Elsevier B.V. All rights reserved.
doi:10.1016/j.jhydrol.2010.03.031

Please cite this article in press as: Luo, L., et al. Quantification of 3-D soil macropore networks in different soil types and land uses using computed tomography. J. Hydrol. (2010), doi:10.1016/j.jhydrol.2010.03.031

macropore networks (e.g., Anderson et al., 1990; Perret et al., 1999, 2000; Luo et al., 2008). Although CT investigations of 2-D macropore characteristics have provided useful information for enhanced understanding of complex soil pore space and related land use impacts (e.g., Gantzer and Anderson, 2002; Udawatta et al., 2008), quantifying macropore features in its true 3-D has been more limited.

Although 3-D visualization of macropores has been realized with algorithms that synthesize 2-D CT images (e.g., Heijs et al., 1995; Mooney and Morris, 2008), quantification of 3-D macropore networks remains a challenge. Various approaches have been used to quantify 3-D macropore geometry and topology. Mathematical morphology (Serra, 1982) has been used to quantify the characteristics of 3-D earthworm burrows using X-ray CT, including pore size distribution, length of each branch, connectivity, and branching intensity (Capowiez et al., 1998; Pierret et al., 2002; Bastardie et al., 2003). Perret et al. (1999) developed a 26-neighbor algorithm to reconstruct the 3-D images of soil macropores in intact soil columns and calculated the number of macropore network, length, tortuosity, hydraulic radius, numerical density of networks, and their connectivity. Lindquist (2002) developed a software package to calculate the 3-D pore size distribution, throat-area distribution, effective throat/pore radii ratios, and pore tortuosity of macropores.

The objectives of this study were to (1) introduce an improved protocol to quantify soil macropore networks based on 3-D X-ray CT images and (2) evaluate the effects of land use and soil type on 3-D soil macropore features. Improvements in our protocol include the length-based macropore parameters such as length density, length distribution, mean hydraulic radius, tortuosity, and angle, which were accurately calculated by skeletonizing 3-D macropores. In this study, macropore size was sorted by actual volume instead of classical assumed equivalent radius. Macropore connectivity was also characterized by quantifying both inter-connectivity (node density) and paths of macropores through the entire soil column (path number), which are more suitable for describing macropores at the column or larger scales, instead of more classical Euler number as an index of connectivity. The variety of 3-D macropore network parameters calculated from our improved protocol, especially when combined with soil functions (see our example application in Luo et al. (submitted for publication)), are essential to understanding macropore impacts on soil properties with different soil types and land uses.

2. Materials and methods

2.1. Soils studied and their sampling

Two soil series with contrasting textures and structures – Hagerstown silt loam (fine, mixed, semiactive, mesic Typic Hapludalfs) and Morrison sand (fine-loamy, mixed, active, mesic Ultic Hapludalfs) – were selected for this study. Both soils are typical in the Ridge and Valley Physiographic Region of Pennsylvania. The sandstone-derived Morrison soils had greater sand content and much higher rock fragments but lower silt and clay contents than the limestone-derived Hagerstown series (Table 1). Two common land uses – cropland and pasture – were selected for each soil series to investigate the impacts by land use. Both cropland sites had conventional tillage and rotation cropping of corn (*Zea mays* L.) and soybean [*Glycine max* (L.) *Merr.*]. Both pasture sites were grazed by animals (cows and horses). Thus, there were four combinations investigated in this study: Hagerstown-cropland (H-C), Hagerstown-pasture (H-P), Morrison-cropland (M-C), and Morrison-pasture (M-P).

Five intact soil columns, 102 mm in diameter and about 350 mm in length, were randomly sampled from each site of the soil series-land use combinations in July 2007. A backhoe was used to carefully push polyvinyl chloride (PVC) pipe (with downward edge sharpened) vertically and gradually into the soil. Three soil horizons were contained in each sampled soil column (Table 1). Detailed procedures of our sampling protocol are described in Luo et al. (2008). Besides the large intact soil columns, three intact small soil cores, 55 mm in diameter and 60 mm in length, were also taken from each soil horizon to measure soil bulk density and saturated hydraulic conductivity in the laboratory. Disturbed soil samples were also taken from each horizon to determine particle size distribution and organic matter content (Table 1). During the soil sampling, each soil profile was also fully described according to standard soil survey procedures.

2.2. X-ray CT scanning

A HD250 Medical Scanner (Universal System, Inc., Solon, Ohio), a 4th-generation system of CT, was used to scan all the soil columns at an energy level of 130 kV and 100 mA. The 512 × 512 images with a voxel size of 0.234 mm × 0.234 mm × 2.000 mm

Table 1
Soil profile description and basic soil properties. The number in parentheses is one standard error ($n = 3$).

Soil and land use (symbol)	Soil horizon	Depth (cm)	Pedality (structure)[a]	Roots[b]	K_{sat}[c] (cm min^{-1})	Bulk density (g cm^{-3})	Sand (%)	Silt (%)	Clay (%)	Organic matter (%)	Rock fragment[d] (%)	Total porosity[e] (cm^3 cm^{-3})
Cropped Hagerstown (H-C)	Ap1	0–15	2 f–m sbk	3 vf–f	0.051 (0.019)	1.34 (0.02)	19	65	16	4.5	1	0.49
	Ap2	15–31	2 m pl parting to 2 m sbk	3 f	0.045 (0.066)	1.35 (0.03)	17	68	15	3.5	2	0.49
	Bt1	31–36+	2 m sbk	2 f	0.035 (0.024)	1.46 (0.02)	23	52	25	1.9	2	0.45
Pastured Hagerstown (H-P)	A1	0–15	3 f–m gr	3 vf–m	0.206 (0.353)	1.16 (0.01)	24	62	13	7.5	1	0.56
	A2	15–32	3 m sbk	3 f	0.363 (0.549)	1.27 (0.00)	24	59	16	3.6	3	0.52
	Bt1	32–36+	2 m sbk	2 f	0.074 (0.010)	1.37 (0.04)	18	62	21	2.0	2	0.48
Cropped Morrison (M-C)	Ap1	0–10	1 f–m sbk	3 vf–f	0.367 (0.461)	1.53 (0.06)	87	9	4	2.0	20	0.42
	Ap2	10–20	1 m sbk	2 f	0.228 (0.034)	1.74 (0.03)	88	9	3	1.3	25	0.34
	Bt1	20–31+	1 m sbk	1 f	0.126 (0.193)	1.77 (0.04)	84	8	9	0.5	25	0.33
Pastured Morrison (M-P)	A1	0–10	1 f–m sbk	3 vf–m	0.357 (0.104)	1.41 (0.04)	73	18	9	4.3	1	0.47
	A2	10–20	1 m sbk	2 f	0.159 (0.084)	1.68 (0.03)	76	14	10	1.2	5	0.37
	Bt1	20–31+	1 m sbk	2 f	0.249 (0.380)	1.69 (0.04)	75	13	12	1.1	5	0.36

[a] Pedality is described using ped grade, ped size and ped shape: 1, 2, 3 for weak, moderate, and strong ped grades, respectively; vf, f, m and c for very fine, fine, medium and coarse ped sizes, respectively; sbk, gr, and pl for subangular blocky, granular and platy ped shapes, respectively.
[b] Roots are described using the quantity and size: 1, 2, 3 for few, common and many, respectively; vf, f, m, c, and vc for very fine, fine, medium, coarse and very coarse root sizes.
[c] Saturated hydraulic conductivity was determined using small soil cores in the lab using constant head method.
[d] Rock fragment (>2 mm in size) content estimated from the computed tomography images.
[e] The porosity was calculated from mean bulk density value (assuming a particle density of 2.65 g cm^{-3}).

Please cite this article in press as: Luo, L., et al. Quantification of 3-D soil macropore networks in different soil types and land uses using computed tomography. J. Hydrol. (2010), doi:10.1016/j.jhydrol.2010.03.031

were produced. Soil water content potentially influences the shape of X-ray attenuation value histogram and possibly the threshold value used for segmenting the images. Since the soil samples from different sites were taken at different times with different initial moisture contents, to minimize the variability among individual soil columns so that the comparison between different soil types and land uses would be more consistent, each column was wetted before scanning by ponding several pore volumes of water at the top of each soil column and draining with the bottom end of each column open to atmosphere for about 3 days. Each soil column thus prepared was assumed to be at approximately field capacity. However, such procedure might produce a gradient in soil water potential along the soil column that could affect the binarization procedure.

2.3. Data processing

Fig. 1 shows the overall procedures of image analysis followed in this study. The images (512 × 512 pixels) were cut to exclude the area outside the soil column using ImageJ version 1.39 (Rasband, 2002). Furthermore, the edge of each soil column was also cut to eliminate any possible artificial features along the edge. The diameter was cut down to 93.7 mm with about 15% of the original cross-sectional area removed. The images were then resampled to 0.3 mm × 0.3 mm × 0.3 mm voxel cubic to facilitate computation. The Lanczos filter in Avizo version 5 (Mercury Computer Systems, Chelmsfold, MA), a widely-used resampling protocol (Meijering et al., 1999), was used to resample all the CT images. In addition, we found that macropore surfaces became much smoother and less jagged after resampling. This step may improve the image quality in the depth direction by interpolating between the original images using Lanczos filter (2-mm slide thickness before resampling). Considering the data size and the computation ability of our computer, the cross-sectional resolution was reduced slightly from 0.234 mm to 0.3 mm after resampling. After that, the median filter, a commonly used image-processing method to reduce the noise while preserving the edge (Jassogne et al., 2007), was used to minimize noise.

The macropore threshold value determined by the maximum entropy threshold algorithm in ImageJ 1.39 was used to segment the images (Jassogne et al., 2007). The threshold value was selected where the inter-class entropy was maximized. The images were also visually inspected to ensure that a reasonable threshold value was used. After segmentation, all macropores <0.75 mm in equivalent cylindrical diameter (ECD) were removed (Luo et al., 2008). Thus, macroporosity in this study specifically refers to the volumetric fraction of pores with equivalent cylindrical diameter ⩾0.75 mm.

After all the soil columns were scanned using CT, the images were carefully examined to identify any soil columns that might have obvious disturbance caused by the sampling (e.g., unnatural macropore morphology). Such soil columns were excluded from further analysis. Sampling disturbance was more likely to occur in the Morrison soil because of its high rock fragment content and weak soil structure (Table 1). Consequently, only four columns each for H-C and H-P, and two columns each for M-C and M-P were selected in the subsequent analysis reported in this paper.

After segmentation, the macropore networks were reconstructed and visualized using Avizo 5. The overall macroporosity, macroporosity distribution along the column depth, macropore volume >1000 mm^3, macropore number, pore size distribution (sorted by macropore volume), mean pore volume, and total surface area were calculated using Avizo 5. Typically, equivalent radius is used to characterize soil macropore size by assuming that the macropore is cylindrical (Hillel, 1998). However, not all macropores are cylindrical and besides equivalent radius, pore length is also critical to its function as a pathway for water, air, and chemical movement. Pore volume, as a parameter of 3-D macropore size, takes into account of both pore width and pore length. Macropores with greater volume are likely more active for flow and transport in soils at near-saturated condition. Therefore, in this study, macropore size was sorted by volume instead of equivalent radius.

Reliable approaches are needed to quantify the continuity, tortuosity, and connectivity of macropores. Since soil macropores are 3-D, skeletonization of macropores is necessary to accurately quantify the topology and length measurements and to effectively visualize the networks in 3-D (Capowiez et al., 1998; Peth et al.,

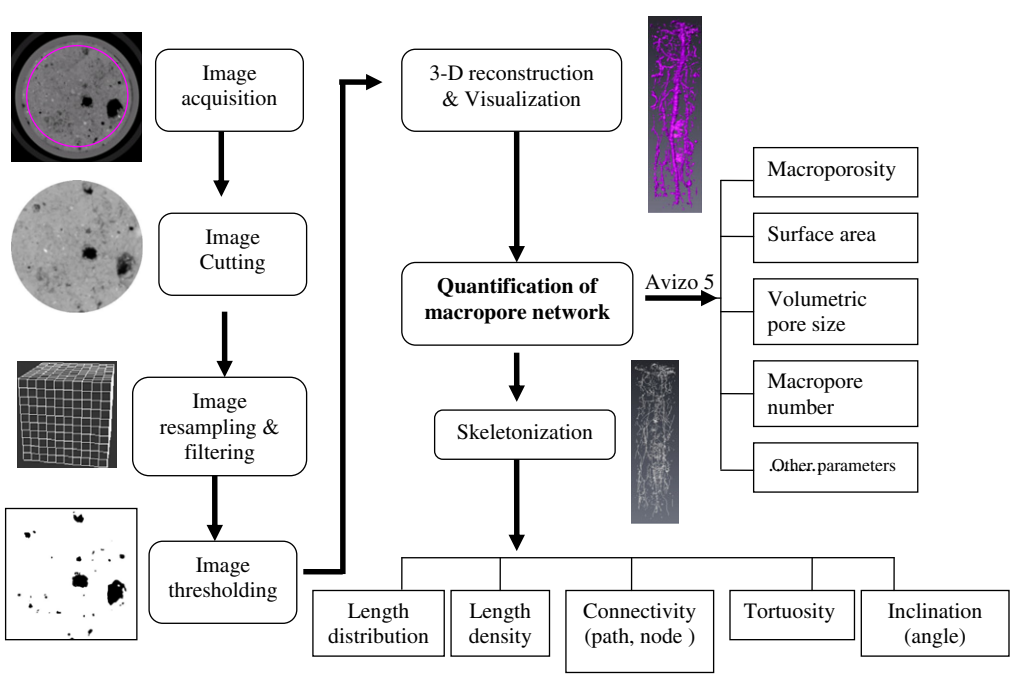

Fig. 1. The procedures used in this study for image analysis and quantification of macropore networks.

Please cite this article in press as: Luo, L., et al. Quantification of 3-D soil macropore networks in different soil types and land uses using computed tomography. J. Hydrol. (2010), doi:10.1016/j.jhydrol.2010.03.031

2008) (Fig. 2a). The skeleton of a macropore is its central line (Fig. 2a), from which the distance is the closest towards more than one boundary points. There are few studies that calculate macropore length and tortuosity based on the skeleton. Pierret et al. (2002) obtained ultimate eroded points from 2-D images and then connected the points from the consecutive images to create 3-D skeletons of macropores. This method is problematic to obtain the skeleton of horizontally-oriented macropores. The skeletonization of highly irregular pores may produce noisy skeletons and cause overestimation of the length (Peth et al., 2008). Lindquist (2002) developed 3DMA software to obtain the skeleton (i.e., median axis) of the pore space. However, skeletons with dead ends were deleted to eliminate the noise in the programming. Since many macropores may have dead ends in large soil columns (Luo et al., 2008), macropore length is likely to be underestimated by 3DMA (Peth et al., 2008). Therefore, the skeletons of macropores with dead ends were included in this study. But for highly irregular macropores (e.g., non-biopores), macropore length could be overestimated due to the noise generated during skeletonization.

The skeletons of macropore networks were generated by determining the nearest distance to the border voxels and thinning based the nearest distance using Avizo 5. After skeletonization, a customized computer program was developed in C to track and quantify each macropore network. One macropore network may consist of several branches of connected macropores or just one individual macropore (Fig. 2). Macropore network density is the number of macropore networks in a unit volume. A node is defined as an intersection where two branches of pores are connected. The number of nodes in each macropore network was recorded. The node density (number m^{-3}) is the number of nodes in a unit volume. For each macropore network, the actual length of the longest path and other branches as well as their positions (starting and ending points) and straight-line distances were also calculated (Fig. 2). The length density (km m^{-3}) is the total actual length of macropores ($\sum L_t$) in a unit volume.

The tortuosity (τ) was calculated as the ratio of the actual macropore length (L_t) to the straight-line distance (L_l) (Fig. 2b):

$$\tau = \frac{L_t}{L_l} \tag{1}$$

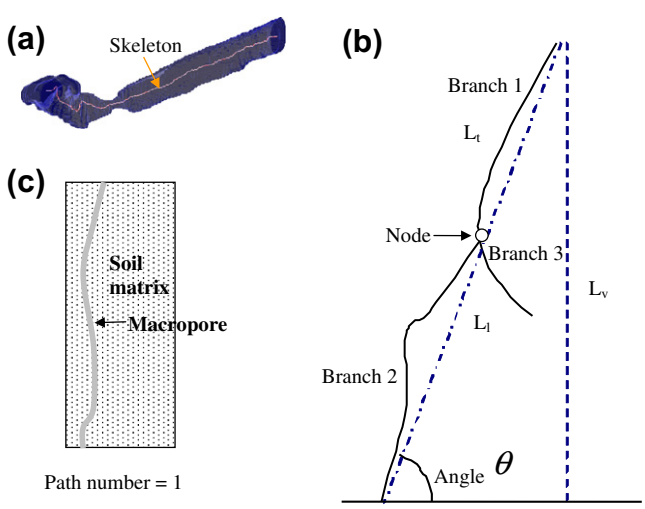

Fig. 2. (a) An example of skeleton of a macropore with different diameters along the length; (b) a macropore network with three branches and one node. The macropore network straight-line length (L_l) is the longest distance through a macropore network (that is, $L_{l\text{-branch1}} + L_{l\text{-branch2}}$); macropore network vertical length (L_v) is equal to $L_{v\text{-branch1}} + L_{v\text{-branch2}}$; total actual macropore network length (L_t) of the macropore is equal to $L_{t\text{-branch1}} + L_{t\text{-branch2}} + L_{t\text{-branch 3}}$; and (c) a path through an entire soil column (i.e., path number = 1).

Meanwhile, the mean tortuosity ($\overline{\tau}$) was calculated as ratio of the total actual macropore length (L_t) to total straight-line distance (L_l) of all the macropores in a certain volume (e.g., the entire soil column):

$$\overline{\tau} = \frac{\sum_{i=1}^{n} L_{ti}}{\sum_{i=1}^{n} L_{li}} \tag{2}$$

where i is the index of a macropore branch and n is the total number of macropore branches. The inclination of a macropore branch was characterized by an angle (θ) away from vertical direction (Fig. 2b). The mean angle was calculated as:

$$\overline{\theta} = \frac{\sum_{i=1}^{n} L_{li}\theta_i}{\sum_{i=1}^{n} L_{li}} \tag{3}$$

Assuming that all macropores are cylindrical, its mean equivalent hydraulic radius was calculated by the total volume V_t and total length L_t of the macropore:

$$\overline{r} = \sqrt{\frac{V_t}{L_t \pi}} \tag{4}$$

The macropore length distribution was analyzed using straight-line length of macropores. Besides the actual length (L_t) and straight-line length (L_l), the vertical length of a macropore network (L_v in Fig. 2) was also considered because it represents the vertical continuity and is important to vertical flow and solute transport along a soil column. Total vertical length of macropores with vertical length >150 mm, as well as their tortuosity and angle, were analyzed to investigate the properties of highly continuous macropores.

Connectivity is a measure of the number of independent paths between two points within the pore space (Perret et al., 1999). To quantify connectivity, two factors need to be considered: (1) pore size, because connectivity is pore size-dependent (generally, the smaller the pores, the greater the connectivity for soils) (Vogel and Roth, 1998); (2) scale or distance between the two points (similarly, the shorter the distance, the higher the possibility of more paths). Vogel (1998, 2000) used the Euler–Poincare characteristic (defined as the number of isolated components minus the total number of redundant connections plus the number of enclosed cavities) to calculate the connectivity function. This method is suitable when the pores are well interconnected, especially at small scale of mm. For macopores at the column and larger scales (cm or larger), most of them are isolated and local redundant connections and enclosed cavities are very small compared with the size of the area of interest (Luo et al., 2008; Noguchi et al., 1999). For such case, the Euler number becomes elusive as an index of connectivity, that is, the number of independent paths between two points or boundaries. Therefore, it is difficult to interpret the results and relate them to soil functional properties, especially when different types of macropores are present in the soils studied. Perret et al. (1999) calculated the connectivity of individual macropore networks in a soil column, which did not suffice to evaluate its effect on the function of the entire soil column. In order to quantify the paths through the entire soil column and inter-connectivity of macropores, the number of independent paths between the two ends of the entire soil column (Fig. 2c) and the node density (number of nodes per unit volume) of the macropore network were determined.

Please cite this article in press as: Luo, L., et al. Quantification of 3-D soil macropore networks in different soil types and land uses using computed tomography. J. Hydrol. (2010), doi:10.1016/j.jhydrol.2010.03.031

2.4. Statistics

All statistical analyses were performed using Minitab version 15 (Minitab Inc., State College, PA). Since the numbers of replicates were not the same for different soil type-land use combinations, the significance tests for the effects of soil type, land use, and their interaction on macropore characteristics were performed using two-way analysis of variance (ANOVA) within the General Linear Model (GLM) procedure. The assumption of homogeneity of variance was made. Within GLM procedure, the Tukey's multicomparison test was used to compare the mean of all soil macropore characteristics among the different soil series-land use combinations.

3. Results and discussion

3.1. Visualization of macropore networks

Three-dimensional visualizations of macropores in the 12 soil columns are shown in Figs. 3 and 4. Macropore characteristics were distinctly different among the different soil type-land use combinations. Different types of macropores could also be observed. The macropores formed by earthworms were highly continuous, relatively large, and tubular. While the macropores formed by roots were also highly continuous and round in shape, their size generally decreased with depth. The smaller and more randomly and less continuously distributed macropore were likely

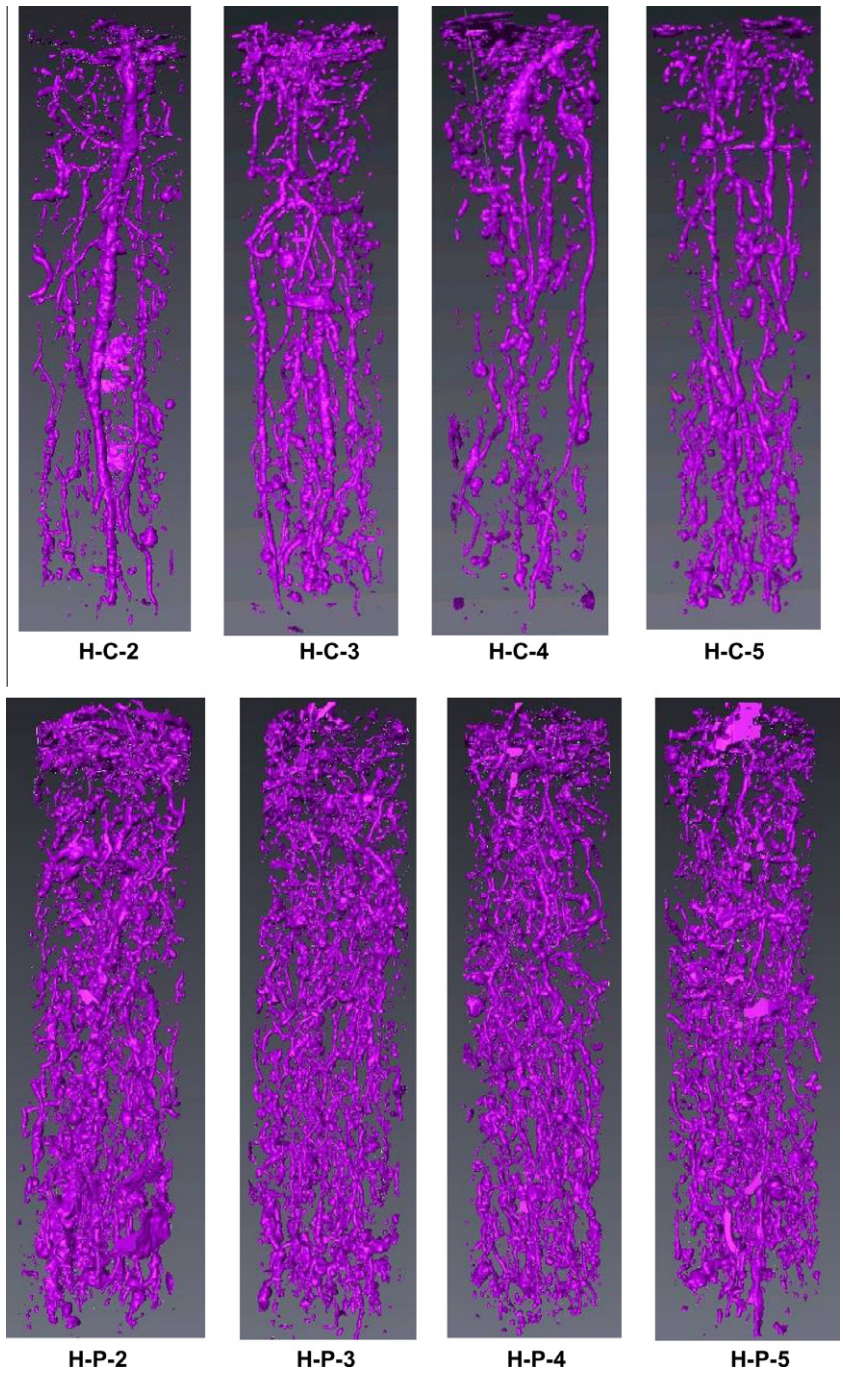

Fig. 3. Three-dimensional visualization of soil macropore networks for the soil columns (94 mm in diameter after cutting and about 350 mm in vertical length) of cropped Hagerstown (H-C, 4 replicates) and pastured Hagerstown (H-P, 4 replicates).

Please cite this article in press as: Luo, L., et al. Quantification of 3-D soil macropore networks in different soil types and land uses using computed tomography. J. Hydrol. (2010), doi:10.1016/j.jhydrol.2010.03.031

inter-aggregate macropores, such as those formed by freezing and thawing or wetting and drying. The macropores formed by earthworm burrows and root channels constituted a significant proportion of the macropore networks in three of the four soil series-land use combinations (except M-C) (Figs. 3 and 4). The macropores for the cropped Hagerstown (H-C) were less abundant compared to that in the pastured Hagerstown (H-P), but were less tortuous and smoother (Fig. 3). We observed an earthworm burrow through the whole column in one of the H-C columns (H-C-2). The greater macroporosity and more tortuous paths in the pastured Hagerstown may be associated with greater competition for food and space among more abundant earthworms in the H-P.

During the soil profile description, we did not observe earthworms in the subsurface of the cropped Morrison soil (but we found earthworms at the other three sites). Thus, the tubular macropores observed in the M-C were likely formed by roots. A number of macropores were observed at the surface in the M-C but were relatively sparse in its subsurface because of fewer biopores and weak aggregation. Compared with the M-C, the M-P contained earthworms and had greater organic matter content and slightly finer texture (Table 1). Many continuous and tubular pores formed by decayed roots of perennial grass were also observed in both the M-P and the H-P.

3.2. Macroporosity, macropore network density, and total surface area

The macropore characteristics of all soil type-land use combinations are listed in Table 2. The mean macroporosity for the H-P was the highest, 0.061 $m^3\ m^{-3}$, over two times of the mean macroporosity for other soil type-land use combinations (0.028 $m^3\ m^{-3}$ for the H-C, 0.024 $m^3\ m^{-3}$ for the M-C, and 0.031 $m^3\ m^{-3}$ for the M-P) (Table 2).

Fig. 5 shows the change of macroporosity along depth in each soil column studied. The general patterns observed in the H-P and M-P were similar, i.e., macroporosity decreased quickly at top 40 mm for the H-P and 60 mm for the M-P, and then increased slowly until about 270-mm depth. The low macroporosity at 40 mm depth for the H-P and 60 mm depth for the M-P was likely associated with the compaction caused by grazing. In comparison, the macroporosity change with depth was significantly different between the H-C and the M-C (Fig. 5). The finer texture and deeper solum of the Hagerstown silt loam were favorable for earthworms. During the sampling, we had observed in situ that organic matter has been taken downward through the earthworm burrows. Below the plow pan, there was less disturbance from agricultural management. Therefore, considerable amount of macroporosity still existed in the subsurface of the H-C. In contrast, the Morrison sand had high sand content, high fraction of rock fragments, and low organic matter content, which were not favorable for earthworms and plant root growth. Therefore, soil macroporosity was low in the M-C subsurface.

Total surface area and macropore network density varied among the different soil type-land use combinations in a way similar to that of macroporosity (Table 2). The correlation analyses showed that macroporosity, total surface area, macropore network density, length density, and node density were highly correlated (Table 3). Such good correlation between macroporosity and connectivity parameters (network density, length density, and node density) may have been partially due to the way we defined macropore size (by volume rather than equivalent pore radius). The H-P had the greatest total surface area for the entire column (141,096 mm^2) and macropore network density (12.84 e+5 number m^{-3}), while the M-C had the lowest (67,147 mm^2 for total surface area and 6.81 e+5 number m^{-3} for macropore network density).

3.3. Macropore size distribution and mean macropore size

Fig. 6 shows the macropore size distribution sorted by volume. The volume percentage of the macropores within certain volume

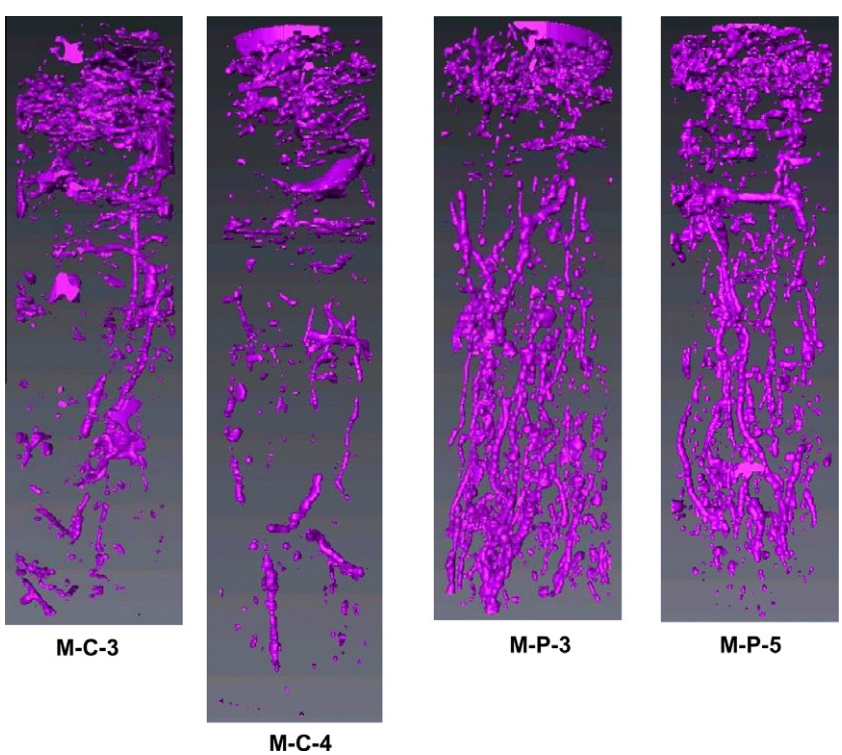

Fig. 4. Three-dimensional visualization of soil macropore networks for the soil columns (94 mm in diameter after cutting and about 350 mm in vertical length) of cropped Morrison (M-C, 2 replicates) and pastured Morrison (M-P, 2 replicates).

Please cite this article in press as: Luo, L., et al. Quantification of 3-D soil macropore networks in different soil types and land uses using computed tomography. J. Hydrol. (2010), doi:10.1016/j.jhydrol.2010.03.031

Table 2
Macropore characteristics of all soil columns as determined from CT images. The number in parentheses is one standard error of the mean. The letters after the parenthesis indicate the significance test of mean difference among the four groups of soil columns at $p < 0.05$.

Soil column	Macro-porosity ($m^3\ m^{-3}$)	Total surface area (mm^2)	POM 1000[a] (%)	Network density ($\times 10^5$) (number m^{-3})	Mean macropore size (mm^3)	Length density (km m^{-3})	Mean tortuosity	Mean angle (°)	Path number	Node density (number m^{-3})	Hydraulic radius (mm)	Length 150[b] (mm)	Tortuosity 150[b]	Angle 150[b] (°)
H-C-2	0.031	65400	62.44	7.97	39.3	5.08	1.56	33.7	1	298,006	0.76	692.7	1.31	9.0
H-C-3	0.031	75554	62.94	8.47	36.3	6.10	1.56	34.6	0	305,601	0.70	207.6	1.40	4.4
H-C-4	0.024	61553	52.37	8.33	28.8	4.99	1.55	39.4	0	303,901	0.68	240.0	1.39	9.8
H-C-5	0.025	60040	45.19	7.51	33.3	4.15	1.46	26.9	0	291,338	0.76	508.2	1.27	5.7
Mean	0.028 (0.002) a	65637 (3492)a	55.74 (4.28) a	8.07 (0.21) bc	34.49 (2.2) a	5.08 (0.40) a	1.53 (0.02) a	33.7 (2.6) a	0 (0) a	299,712 (3230) a	0.72 (0.02) a	412.1 (115.3) a	1.34 (0.03) a	7.2 (1.4) a
H-P-2	0.074	147932	71.19	12.36	59.6	12.93	1.87	40.3	0	513,233	0.74	189.9	1.67	12.5
H-P-3	0.060	144866	64.06	13.73	43.4	12.93	1.82	37.1	0	584,611	0.67	179.7	1.56	0.9
H-P-4	0.055	138821	59.04	13.18	41.5	11.19	1.70	37.1	0	540,131	0.69	517.8	1.33	11.8
H-P-5	0.056	132765	52.65	12.07	46.3	10.24	1.59	35.0	0	531,338	0.72	152.1	2.24	14.3
Mean	0.061 (0.004) b	141096 (3360) b	61.73 (3.92) a	12.84 (0.80) a	47.7 (4.1) b	11.82 (0.67) b	1.75 (0.06) ab	37.4a (2.1)	0 (0) a	542,328 (15,165) b	0.70 (0.02) a	259.9 (86.3) a	1.70 (0.19) a	9.9 (3.0) a
M-C-3	0.026	63764	67.61	7.01	37.5	4.47	1.73	61.6	0	187,099	0.75	0	N/A	N/A
M-C-4	0.022	57322	59.18	6.61	32.5	4.87	1.91	57.7	0	187,124	0.66	0	N/A	N/A
Mean	0.024 (0.002) a	60543 (3221) a	63.39 (4.2) a	6.81 (0.20) b	35.0 (2.5) ab	4.67 (0.2) a	1.82 (0.09) b	59.7 (1.95) b	0 (0) a	187,112 (13) c	0.70 (0.05) a	0 (0) a	N/A	N/A
M-P-3	0.031	66319	44.83	8.76	35.8	4.50	1.56	35.8	0	239,151	0.81	0	N/A	N/A
M-P-5	0.032	67974	65.54	9.16	34.4	4.99	1.67	40.9	0	256,326	0.78	198.3	1.97	19.4
Mean	0.031 (0.001) a	67147 (828) a	55.18 (10.35) a	8.96 (0.20) c	35.1 (0.7) ab	4.74 (0.25) a	1.62 (0.06) ab	38.4a (2.6)	0 (0) a	247,739 (8587) ac	0.80 (0.02) a	99.2 (99.2) a	N/A	N/A

[a] POM1000 is the proportion of macropores with volume >1000 mm^3.
[b] Length 150, tortuosity 150, and angle 150 are the total vertical length, mean tortuosity, and mean angle for macropores with vertical length >150 mm. For some Morrison sand columns, no macropores with vertical length >150 mm were available, thus no corresponding tortuosity and angle data available.

Please cite this article in press as: Luo, L., et al. Quantification of 3-D soil macropore networks in different soil types and land uses using computed tomography. J. Hydrol. (2010), doi:10.1016/j.jhydrol.2010.03.031

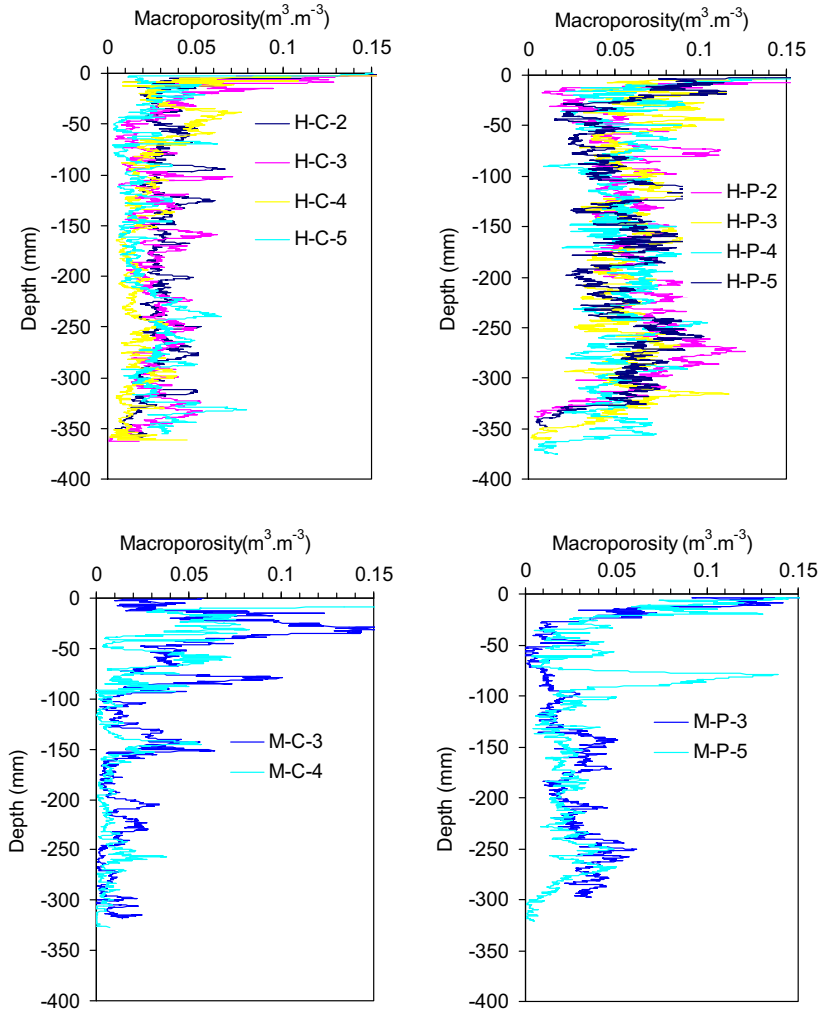

Fig. 5. Macroporosity distribution along the soil column depth for cropped Hagerstown (H-C, 4 replicates), pastured Hagerstown (H-P, 4 replicates), cropped Morrison (M-C, 2 replicates), and pastured Morrison (M-P, 2 replicates).

range to total soil volume was calculated. Within the same soil type and land use, the macropore size distributions were about the same for macropores with volume < 100 mm^3, and the difference increased with macropore size (Fig. 6). More than 50% of the macropore volume consisted of macropores with volume >1000 mm^3 for all soil columns (55.7% for H-C, 61.7% for H-P, 63.4% for M-C, and 55.1% for M-P) (Table 2). These large macropores were likely biopores. The H-P, with the greatest macroporosity (0.061 $m^3\,m^{-3}$), also had the largest mean macropore size (46.3 mm^3 on average), while the other three soil type-land use combinations had similar overall macroporosity (0.024–0.031 $m^3\,m^{-3}$) and mean macropore volume (~35 mm^3) (Table 2). As expected, the greater the macroporosity, the greater the chance for macropores to be interconnected and to form bigger macropores.

3.4. Macropore length density and length distribution

Macropore length density was calculated based on the skeletons of macropores (Fig. 7). As expected, mean macropore length density for the H-P was the highest, 11.82 km m^{-3}, about twice that of the H-C (5.08 km m^{-3}). Mean macropore length density for the M-P and the M-C were 4.74 km m^{-3} and 4.67 km m^{-3}, respectively (Table 2). Because of highly irregular pores at the top of the M-C, the skeletons produced might be noisy and cause the overestimation of its length density. Generally, length density of the Hagerstown soils was greater than that of the Morrison soils.

The macropores were also sorted by their vertical length (Fig. 8). Although the H-C did not have the highest macropore length density, three of its columns (H-C-2, H-C-3, and H-C-5) had the highest total vertical length of the macropores with vertical length >90 mm (Fig. 8). The columns of the H-C, H-P, and M-P had 412.1, 259.9, and 99.2 mm mean total vertical length of the macropores with vertical length >150 mm, respectively, while the M-C had no macropore longer than 150 mm. These results are consistent with the macropore morphology shown in Figs. 3 and 4. The highly continuous macropores are potentially active in hydrological processes at near-saturated conditions and are critical to preferential flow and transport, as illustrated in Luo et al. (submitted for publication).

3.5. Macropore tortuosity, inclination, and connectivity

Mean tortuosity was 1.53, 1.75, 1.82, and 1.62 for the H-C, H-P, M-C, and M-P, respectively (Table 2). The highly continuous macropores (e.g., macropores with vertical length >60 mm) in the H-C had the mean tortuosity of 1.32–1.34, while that for the H-P and the M-P was 1.50–1.71 and 1.32–1.64, respectively. As indicated in Figs. 3, 4 and 9, highly continuous macropores were likely biopores, which had relatively low tortuosity. For example, the tor-

Table 3
Pearson correlation coefficient among different macropore characteristics as determined from CT images for all the soil columns studied. Probability values in parentheses are indicated by two significance levels (** <0.01, * <0.05).

Properties	Total surface area C1	Macro-porosity C2	POM1000[a] C3	Network density C4	Mean pore size C5	Length density C6	Mean tortuosity C7	Mean angle C8	Path number C9	Node density C10	Hydraulic radius C11	Length 150[b] C12	Tortuosity 150[b] C13
C2	**0.97 (0.00 **)**												
C3	0.32(0.31)	0.37(0.23)											
C4	**0.96(0.00 **)**	**0.92(0.00**)**	0.20(0.53)										
C5	**0.82(0.00 **)**	**0.92(0.00**)**	0.48(0.11)	**0.69(0.01**)**									
C6	**0.99(0.00**)**	**0.96(0.00**)**	0.38 (0.22)	**0.95(0.00**)**	**0.82(0.00**)**								
C7	0.43(0.17)	0.43(0.16)	**0.66(0.02*)**	0.27(0.41)	0.45(0.14)	0.50(0.10)							
C8	−0.36(0.26)	−0.38(0.23)	0.39(0.21)	−0.52(0.09)	−0.24(0.46)	−0.32(0.32)	**0.58(0.05*)**						
C9	−0.21(0.52)	−0.14(0.68)	0.13(0.69)	−0.16(0.62)	0.01(0.97)	−0.19(0.55)	−0.23(0.47)	−0.16(0.62)					
C10	**0.96(0.00 **)**	**0.91(0.00**)**	0.17(0.17)	**0.99(0.00**)**	**0.70(0.01**)**	**0.95(0.00**)**	0.23(0.47)	−0.54(0.07)	−0.12(0.71)				
C11	−0.30(0.34)	−0.14(0.65)	−0.20(0.53)	−0.31(0.33)	0.04(0.90)	−0.38(0.22)	−0.44(0.16)	−0.24(0.44)	0.24(0.45)	−0.34(0.28)			
C12	0.06(0.85)	0.06(0.87)	−0.08(0.81)	0.19(0.56)	0.02(0.96)	0.05(0.88)	−0.43(0.16)	**−0.57(0.05*)**	**0.64(0.03*)**	0.24(0.45)	0.07(0.84)		
C13	0.31(0.42)	0.35(0.36)	0.16(0.68)	0.24(0.54)	0.32(0.39)	0.25(0.52)	0.25(0.52)	0.18(0.65)	−0.29(0.46)	0.24(0.54)	0.27(0.48)	−0.63(0.07)	
C14	−0.02(0.97)	0.07(0.86)	0.15(0.70)	−0.09(0.82)	0.12(0.76)	−0.09(0.82)	0.08(0.83)	0.46(0.21)	−0.05(0.89)	−0.13(0.73)	0.54(0.13)	−0.12(0.75)	0.65(0.06)

[a] POM1000 is the proportion of macropores with volume >1000 mm^3.
[b] Length 150, tortuosity 150, and angle 150 are the total vertical length, mean tortuosity, and mean angle for macropores with vertical length >150 mm; C14 is for angle 150.

tuosity of the earthworm burrow through the H-C-2 column was about 1.33. On the other hand, the tortuosity of the M-C was higher than other columns because of fewer biopores. The tortuosity value calculated in this study is larger than that calculated by Perret et al. (1999) (1.12–1.17) but comparable with that of Jassogne et al. (2007) (1.5–2.5).

The macropores of the H-C had a mean angle of 33.7°, suggesting that the macropores were largely vertically oriented. This was partly due to the large proportion of vertically oriented earthworm burrows and roots. In contrast, the macropores of the M-C had a much greater mean angle of 59.7° than any other soil type-land use combinations. The mean angles for the H-P and the M-P were 37.4° and 38.4°, respectively (Table 2). Fig. 10 shows the change of mean angle with macropore vertical length. In general, the macropores with greater vertical length tended to have smaller angle (i.e., more vertically oriented).

The node density varied among the soil type-land use combinations in a similar way as the macroporosity and macropore length density. The greater the macroporosity, the greater the node density (Table 3), indicating a higher inter-connectivity among macropores. Among all the soil columns studied, only the soil column H-C-2 had a macropore network (earthworm burrow) that was continuous throughout the entire column, so its path number was 1. The rest of the soil columns had no macropore passing through the entire column, so their path number was all zero.

3.6. Effects of soil type and land use on macropore characteristics

The analysis of variance indicated that soil type, land use, and their interaction had significant impacts on macroporosity, total surface area, macropore network density, length density, node density (inter-connectivity), and mean angle (inclination), but not on the proportion of macropores with volume >1000 mm^3, path number, and total length of macropores with vertical length >150 mm (Table 4). Only the interaction of soil type and land use influenced mean tortuosity and mean hydraulic radius (Table 4). The interaction of soil type and land use indicated that the influence of soil type on macropore characteristics varied with land use, and vice versa.

Within the same land use, the Morrison sand had lower macroporosity, total surface area, macropore network density, pore length density, and node density than the Hagerstown silt loam (Table 2). For the Hagerstown silt loam, mean macroporosity, total surface area, macropore network density, pore length density, and node density was 0.045 m^3 m^{-3}, 10,3366 mm^2, 10.45+e5 number m^{-3}, 8.45 km m^{-3}, and 42,1019 number m^{-3}, respectively, which were about 1.60, 1.61, 1.32, 1.79, and 1.93 times greater than those of the Morrison sand, respectively. The macropores for the Hagerstown silt loam was more vertically oriented (35.5° mean angle) than that of the Morrison sand (49.0° mean angle). The Hagerstown silt loam had finer texture, better structure, higher organic matter content, and lower rock fragment content throughout the profile as compared to the Morrison sand (Table 1). Consequently, the Hagerstown silt loam was more fertile for plant growth and more favorable for fauna activities than the Morrison sand. The greater biological activities in the Hagerstown silt loam led to more abundant biopores.

Within the same soil type, macropore characteristics were altered by land uses. Our results showed that the soils with pasture land use had greater macroporosity, total surface area, macropore network density, pore length density, and node density than those with crop land use. Mean macroporosity, total surface area, macropore network density, pore length density, and node density was 0.051 m^3 m^{-3}, 11,6446 mm^2, 11.54+e5 number m^{-3}, 9.46 km m^{-3}, and 44,4131 number m^{-3}, respectively, for the soils in pasture, which were about 1.93, 1.82, 1.51, 1.91, and 1.69 times higher than

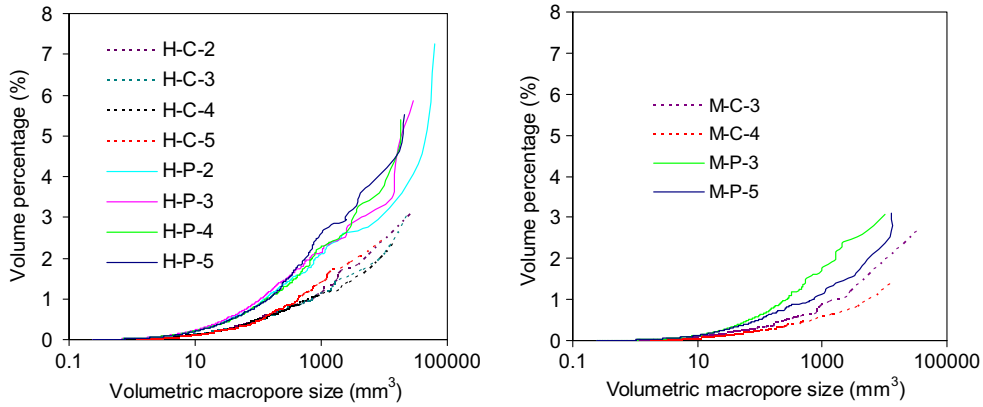

Fig. 6. Cumulative macropore size distribution (by volume) in the soil columns of cropped Hagerstown (H-C, 4 replicates), pastured Hagerstown (H-P, 4 replicates), cropped Morrison (M-C, 2 replicates), and pastured Morrison (M-P, 2 replicates).

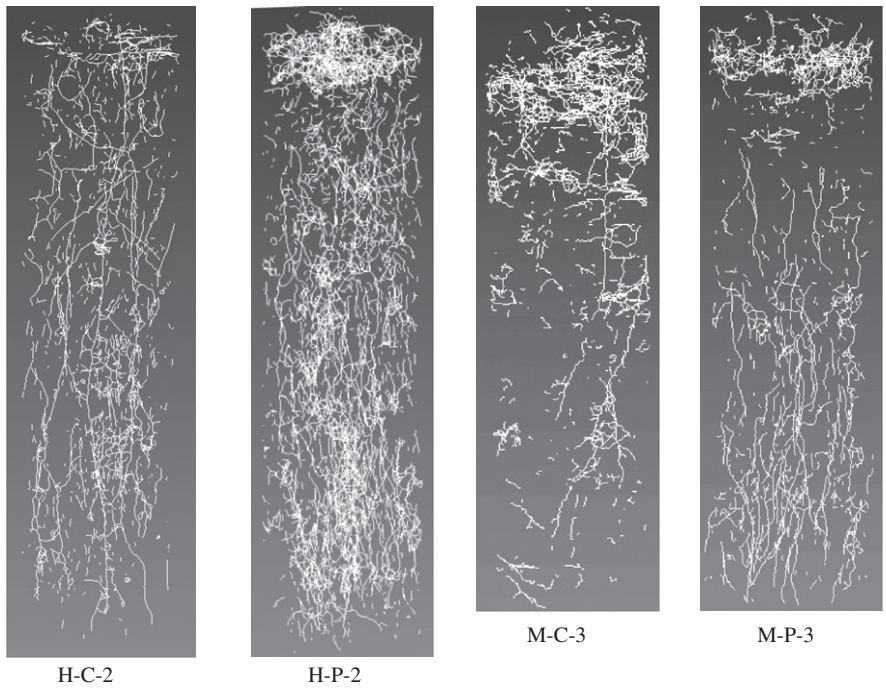

Fig. 7. Representative skeletons of the soil macropore networks in the soil columns of cropped Hagerstown (H-C), pastured Hagerstown (H-P), cropped Morrison (M-C), and pastured Morrison (M-P). Each column is 94 mm in diameter (after image cutting) and about 350 mm in vertical length.

those in cropland, respectively. Overall, macropores in the pasture lands were more also vertically inclined (37.7° mean angle) than that in the cropped lands (42.3° mean angle). The greater accumulation of organic matter and more fauna activities in the pasture land use have contributed to the greater abundance and higher connectivity of macropores. A significant positive correlation was found between the organic matter content and the macroporosity of each horizon in all the soil columns studied ($r^2 = 0.61$, $p < 0.01$). The perennial grass in the pasture land produced abundant living and decayed roots, which contributed to the organic matter accumulation in the soils (Table 1) and provided main source of food for soil biota. Thus, high proportion of biopores was observed in the H-P and M-P as compared to their cropland counterparts.

The differences in macropore characteristics among the different soil types and land uses imply that the soil functional properties would be different among the two soil types and land uses studied. Previous studies have reported that although macropres constitute only a small fraction of total soil porosity, macropores may dominate near-saturated flow (Beven and Germann, 1982; Perret et al., 2000). Because of the high flow rate in macropores, contaminants in macroporous soils may quickly bypass the soil matrix and reach groundwater. From our results, it is expected that macropores would generally play a more prominent role in flow and transport in the Hagerstown soils and under pasture land use, as compared to the Morrison soils and under row crop. During drainage, fresh air would also enter into the soil more rapidly and enhance aeration for biological activities in the Hagerstown soils and under pasture, which would provide a positive feedback to further macropore developments in this soil and land use.

4. Summary and conclusions

The approach proposed in this study allowed a detailed characterization of diverse morphological features of 3-D macropore networks reconstructed from X-ray CT images. A suite of macropore parameters were quantified for a total of 12 intact soil columns that demonstrated the impacts from soil types and land uses.

Please cite this article in press as: Luo, L., et al. Quantification of 3-D soil macropore networks in different soil types and land uses using computed tomography. J. Hydrol. (2010), doi:10.1016/j.jhydrol.2010.03.031

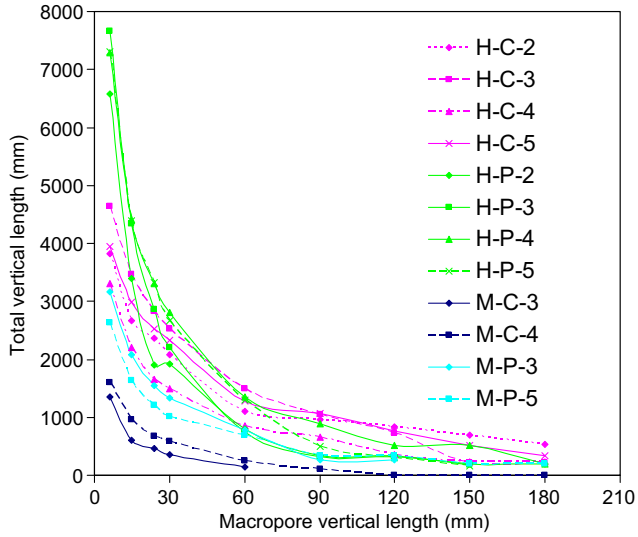

Fig. 8. Macropore vertical length distributions in the soil columns of cropped Hagerstown (H-C, 4 replicates), pastured Hagerstown (H-P, 4 replicates), cropped Morrison (M-C, 2 replicates), and pastured Morrison (M-P, 2 replicates).

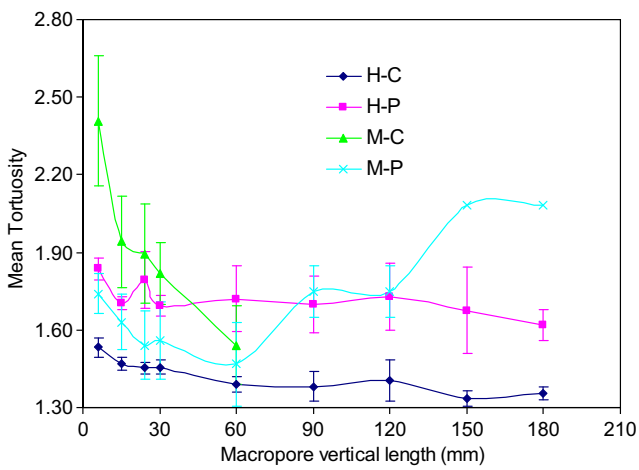

Fig. 9. Distribution of mean tortuosity vs. macropore vertical length for the soil columns of cropped Hagerstown (H-C), pastured Hagerstown (H-P), cropped Morrison (M-C), and pastured Morrison (M-P).

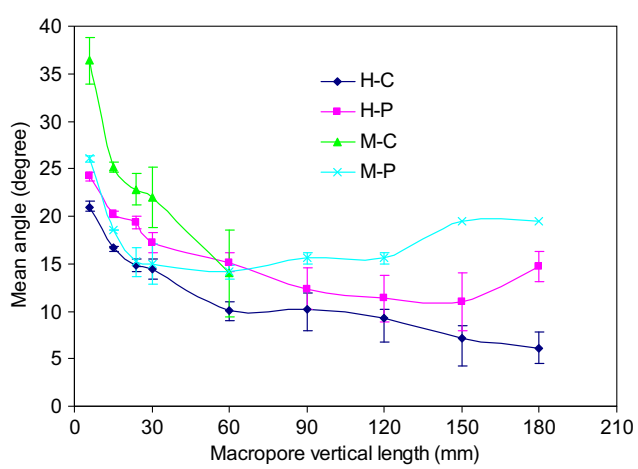

Fig. 10. Distribution of mean macropore angle vs. macropore vertical length for the soil columns of cropped Hagerstown (H-C), pastured Hagerstown (H-P), cropped Morrison (M-C), and pastured Morrison (M-P).

Table 4
Analysis of variance of soil macropore characteristics as determined from CT images, and the effects of soil type, land use, and their interactions on macropore characteristics. MS is mean square of the effect. Values of p are indicated using three significance levels (*** $p<0.01$, ** $p<0.05$, * $p<0.1$).

Effect	Total surface area (mm^2)		Macroporosity ($m^3\ m^{-3}$)		POM1000[a] (%)		Network density (number m^{-3})		Mean pore size (mm^3)		Length density (km m^{-3})	
	MS	*p*	*MS*	*p*	*MS*	*p*	*MS*	*p*	*MS*	*p*	*MS*	*p*
Soil	4.17E+09	0.000***	7.432E−04	0.002***	0.8	0.923	17,93,613	0.000***	96	0.134	37.34	0.000***
Land use	4.49E+09	0.000***	1.105E−03	0.001***	3.3	0.847	17,94,707	0.000***	119	0.101	30.96	0.000***
Soil * land use	3.16E+09	0.000***	4.373E−04	0.008***	134.6	0.235	314,417	0.006***	116	0.104	29.64	0.000***
Effect	Mean tortuosity		Mean angle (°)		Path (number)		Node density (number m^{-3})		Hydraulic radius (mm)		Length 150[b]	
	MS	*p*	*MS*	*p*	*MS*	*p*	*MS*	*p*	*MS*	*p*	*MS*	*p*
Soil	0.016	0.230	355.5	0.000***	0.042	0.524	1.11E+11	0.000***	0.003	0.198	2.43E+06	0.034**
Land use	0.000	0.900	199.8	0.001***	0.042	0.524	6.13E+10	0.000***	0.004	0.174	2.09E+04	0.819
Soil * land use	0.114	0.009***	218.4	0.001***	0.042	0.524	2.21E+10	0.000***	0.009	0.048**	4.68E+05	0.295

[a] POM1000 is the proportion of macropores with volume >1000 mm^3.
[b] Length 150 is the total vertical length, mean tortuosity, and mean angle for macropores with vertical length >150 mm.

Among various macropore characteristics, macroporosity, total surface area, macropore network density, length density, and node density were positively correlated with each other across soil types and land uses. In comparison, mean pore size, tortuosity, path number, hydraulic radius were more independent of each other. Skeletonization of 3-D macropore networks improved the quantification of length-based macropore parameters and made it easier to visualize pore topology. However, macropore length, especially for macropores at the soil surface might be overestimated because the skeletons of macropores with dead ends were kept, which could be noise generated during skeletonization. An improved algorithm that deletes the noise while maintaining the real macropore skeletons is required for future studies.

Our results demonstrated clear distinction in macropore characteristics between the two soil types and two lands uses. Both soil type and land use had noticeable influences on macroporosity, surface area, macropore network density, length density, node density (inter-connectivity), and mean angle (inclination). Within the same soil series, pasture improved soil macroporosity and macropore network structures, as compared to row crop, especially in the subsoil. Within the same land use, the sandy Morrison soils had fewer macropores and weaker structure than the silt loam Hagerstown soils because of their different suitabilities for plant growth and biota activities. Biological factors significantly alter the soil structural differences and influence flow and transport through generating macropore features in soils.

Because of relatively high variation in macropore characteristics encountered in this study, more replicates for each soil type-land use combination might be needed to draw a firmer conclusion about the difference in their macropore characteristics and related functions. Nevertheless, it is apparent from this study that soil type and land use have obvious impacts on 3-D macropore networks and that both soil type and land use need to be considered simultaneously in order to more fully characterize the causes of macropore variability. Soil type alone is insufficient to separate macropore features and related soil properties if different land uses are encountered. Hence, the concepts of "geneform" (for genetically defined soil series) and "phenoform" (for soil types resulting from a particular form of management within a given genoform) (Droogers and Bouma, 1997) could be used to help distinguish major land uses and management types within the same soil series.

Macropore geometry and distribution is essential when modeling non-equilibrium flow and transport. Spatial distribution of macropores along depth also influences the potential for non-equilibrium flow and transport in field soils. It is expected that physical, chemical, and biological impacts of macropores will be enhanced with an increase in macroporosity, surface area, size, network density, length density, connectivity, and decrease in vertical angle and tortuosity. These 3-D macropore characteristics can be linked to soil functional properties to better understand soil processes and related management practices. We have developed some of quantitative relationship between 3-D macropore characteristics (as quantified in this study) and soil hydraulic functions in a separated paper (see Luo et al., submitted for publication).

Acknowledgements

We thank Dr. Avrami Grader and Dr. Phil Halleck of the Penn State's Center for Quantitative Imaging for their help and advice on the CT scanning. This work was partially supported by the USDA National Research Initiative (Grant # 2002-35102-12547) and the USDA Higher Education Challenge Competitive Grants Program (Grant # 2006-38411-17202).

References

Anderson, S.H., Peyton, R.L., Gantzer, C.J., 1990. Evaluation of constructed and natural soil macropores using X-ray computed-tomography. Geoderma 46, 13–29.

Bastardie, F., Capowiez, Y., Dreuzy, J.-R., Cluzeau, D., 2003. X-ray tomographic and hydraulic characterization of burrowing by three earthworm species in repacked soil cores. Appl. Soil Ecol. 24, 3–16.

Beven, K., Germann, P., 1982. Macropores and water flow in soils. Water Resour. Res. 18, 1311–1325.

Capowiez, Y., Pierret, A., Daniel, O., Monestiez, P., Kretzschmar, A., 1998. 3D skeleton reconstructions of natural earthworm burrow systems using CAT scan images of soil cores. Biol. Fertil. Soils 27 (1), 51–59.

Droogers, P., Bouma, J., 1997. Soil survey input in exploratory modeling of sustainable soil management practices. Soil Sci. Soc. Am. J. 61, 1704–1710.

Gantzer, C.J., Anderson, S.H., 2002. Computed tomographic measurement of macroporosity in chisel-disk and no-tillage seedbeds. Soil Tillage Res. 64 (1–2), 101–111.

Hillel, D., 1998. Environmental Soil Physics. Academic Press, San Diego, CA. p. 120.

Heijs, A.W.J., Delange, J., Scoute, J.F.T., Bouma, J., 1995. Computed tomography as a tool for nondestructive analysis of flow patterns in macroporous clay soils. Geoderma 64, 183–196.

Jarvis, N.J., 2007. A review of non-equilibrium water flow and solute transport in soil macropores: principles, controlling factors and consequences for water quality. Eur. J. Soil Sci. 58, 523–546.

Jassogne, L., McNeill, A., Chittleborough, D., 2007. 3D-visualization and analysis of macro- and meso-porosity of the upper horizons of a sodic, texture-contrast soil. Eur. J. Soil Sci. 58, 589–598.

Lin, H.S., McInnes, K.J., Wilding, L.P., Hallmark, C.T., 1996. Effective porosity and flow rate with infiltration at low tensions into a well-structured subsoil. Trans. ASAE 39, 131–135.

Lin, H.S., Bouma, J., Wilding, L., Richardson, J., Kutílek, M., Nielsen, D., 2005. Advances in hydropedology. Adv. Agron. 85, 1–90.

Lindquist, W.B., 2002. Network flow model studies and 3D pore structure. Contemp. Math. 295, 355–366.

Luo, L.F., Lin, H.S., Halleck, P., 2008. Quantifying soil structure and preferential flow in intact soil using X-ray computed tomography. Soil Sci. Soc. Am. J. 72, 1058–1069.

Luo, L.F., Lin, H.S., Schmidt, J., submitted for publication. Quantitative relationships between soil macropore characteristics and preferential flow and transport. Soil Sci. Soc. Am. J.

Meijering, E.H.W., Niessen, W.J., Pluim, J.P.W., Viergever, M.A., 1999. Quantitative comparison of sinc-approximating kernels for medical image interpolation. In: Medical Image Computing and Computer-Assisted Intervention, MICCAI'99, Proceedings, vol. 1679, pp. 210–217.

Mooney, S.J., Morris, C., 2008. Morphological approach to understanding preferential flow using image analysis with dye tracers and X-ray computed tomography. Catena 73, 204–211.

Noguchi, S., Tsuboyama, Y., Sidle, R.C., Hosoda, I., 1999. Morphological characteristics of macropores and the distribution of preferential flow pathways in a forested slope segment. Soil Sci. Soc. Am. J. 63, 1413–1423.

Perret, J., Prasher, S.O., Kantzas, A., Langford, C., 1999. Three-dimensional quantification of macropore networks in undisturbed soil cores. Soil Sci. Soc. Am. J. 63 (6), 1530–1543.

Perret, J., Prasher, S.O., Kantzas, A., Langford, C., 2000. A two-domain approach using CAT scanning to model solute transport in soil. J. Environ. Qual. 29 (3), 995–1010.

Peth, S., Horn, R., Beckmann, F., Donath, T., Fischer, J., Smucker, A.J.M., 2008. Three-dimensional quantification of intra-aggregate pore-space features using synchrotron-radiation-based microtomography. Soil Sci. Soc. Am. J. 72, 897–907.

Pierret, A., Capowiez, Y., Belzunces, L., et al., 2002. 3D reconstruction and quantification of macropores using X-ray computed tomography and image analysis. Geoderma 106, 247–271.

Rasband, W., 2002. ImageJ: Image processing and analysis in Java (Online). Available at Research Services Branch, National Institute of Health. Bethesda, MD, USA. <http://rsb.info.nih.gov/ij/index.html>.

Serra, J., 1982. Image Analysis and Mathematical Morphology. Academic Press, London.

Udawatta, R.R., Anderson, S.H., Gantzer, C.J., et al., 2008. Influence of prairie restoration on CT-measured soil pore characteristics. J. Environ. Qual. 37, 219–228.

Vogel, H.J., 2000. A numerical experiment on pore size, pore connectivity, water retention, permeability, and solute transport using network models. Eur. J. Soil Sci. 51, 99–105.

Vogel, H.J., Roth, K., 1998. A new approach for determining effective soil hydraulic functions. Eur. J. Soil Sci. 49, 547–556.

Zhou, X., Lin, H.S., White, E.A., 2008. Surface soil hydraulic properties in four soil series under different land uses and their temporal changes. Catena 73, 180–188.